Blind deconvolution of Gaussian blurred images containing additive white Gaussian noise

Philip E. Robinson and Yuko Roodt
Faculty of Engineering and the Built Environment
University of Johannesburg
South Africa
philipr@uj.ac.za, yukor@uj.ac.za

Abstract—**Image restoration algorithms are used to reconstruct the information that is suppressed when an observed image is subjected to blurring. These algorithms generally assume that knowledge of the nature of the distortion and noise contained in an observed image is available. When this information is not available and has to be directly estimated from the image being processed the problem becomes one of blind deconvolution. This paper makes use of a novel blur identification technique and a noise identification technique to perform blind deconvolution on single images that have been degraded by a Gaussian blur and contain additive white Gaussian noise.**

Keywords-blind deconvolution, Gaussian blur, blur detection, noise detection

I. INTRODUCTION

Blur is a phenomenon that can be observed in all real-world vision systems. The effects of blur can be described as a degradation of spatial detail or the high frequency visual information contained in an image. This results in a loss of edge sharpness and the finer structures of a scene. Blur can be caused by many factors but the most fundamental is the diffraction limit of a vision system that contains an aperture [1]. Other well known sources of blurring are defocus, motion during exposure, atmospheric turbulence and upscaling images [1, 2, 3].

Building a real-world imaging system that can capture arbitrarily sharp images is not possible, but it is mathematically possible to reconstruct information that is suppressed by blurring from degraded image data [4]. This process is called image deconvolution or image restoration and is an example of inverse filtering [5]. This process models the blurring distortion as a convolution kernel or point spread function (PSF) that is spatially invariant and is convolved with the undistorted image. The model usually includes an additive white Gaussian noise term to model noise introduced into the scene by the image capture sensor [6]. Assuming that the PSF of the blurring function is known an operation that is the inverse of that PSF is performed on the degraded image to reverse the effects of the distortion [4, 5, 6].

The deconvolution approach to image restoration has been quite thoroughly explored in the literature. The fundamental theory of inverse filtering, least squares filtering and iterative filtering can be found in the majority of image processing textbooks [5, 6, 7] and some more modern approaches have been discussed in the following articles [8, 9, 10].

When the PSF of the blur and the noise characteristics of a given scene are not known the problem becomes one of blind deconvolution [5]. In this case the nature of the blur and noise present in the scene needs to be estimated from the observed degraded image. In this paper we will focus on the blind deconvolution of images that are blurred with a Gaussian kernel and additive white Gaussian noise (AWGN). Gaussian blur is a good approximation of the lack of high frequency information in an image upsampled using bilinear and bicubic interpolation as is the case in single-frame super resolution [11]. A Gaussian blur is also a good approximation for the blur caused by imaging through atmospheric turbulence [5].

In this work we will make use of the novel Gaussian blur identification algorithm we proposed in [12] to estimate the blur contained in an image. This is a very naïve technique that makes use of an interesting feature of the Gaussian function to accurately estimate Gaussian blur applied to an image. This is done without any knowledge of the contents of the image or other prior assumptions that the majority of methods in the literature require. Together with a noise estimation technique we use these estimates to perform single-frame blind deconvolution for the purpose of image restoration.

The literature contains a huge amount of research regarding blind deconvolution of images containing various kinds of blurs. The vast majority of these techniques make use of statistical techniques using a variety of priors. Maximum a posteriori probability techniques are explored in [13]. In [14] a form of regularization is employed. The blurring function that has been applied to an image can also be treated as a autoregressive–moving-average (ARMA) process as is done in [15]. A survey of the main archetypes of blind deconvolution approaches can be found in [16]. This survey shows a number of unconventional approaches to the problem such as making use of parametric models of a blurring function.

The remainder of this paper will be structured as follows. Section II will describe the deconvolution model used in this paper. Section III will describe the blur identification technique that was employed. Section IV will describe the noise identification technique that was chosen. Section V will discuss the final integration of the various elements of the algorithm.

Section VI will present the results achieved using the algorithm and finally Section VI will be the conclusion.

II. DECONVOLUTION MODEL

The model that is typically used to describe the composition of a blurred image is shown by the following equation.

$$i(x,y) = f(x,y) * h(x,y) + n(x,y), \quad (1)$$

Where *i(x,y)* is the distorted 2D image with the 2 spatial dimensions denoted by *x* and *y, f(x,y)* is the undistorted image, *h(x,y)* is the blurring function PSF which is convolved with the input image and *n(x,y)* is the additive white Gaussian noise present in the scene [5, 6]. The primary cause of the presence of noise in digital images is thermal sensor noise and is dependent on exposure levels and gain used during image capture.

We employ the classic Wiener or least square error filtering approach for deconvolution. This approach is an inverse filtering scheme that takes into account the power of the noise present in the distorted frame. This approach is better at handling the case where there are zeros in the distorting PSF [5, 6]. The following equation describes the Wiener filtering scheme.

$$H_w = \frac{H^*}{|H|^2 + S_N/S_F}, \quad (2)$$

Where S_N is the power spectrum of the additive noise, S_F is the power spectrum of undistorted the image, H is the frequency-domain model of the distortion and H_w is the Wiener Filter based on the specified model.

The goal of this paper is to estimate the blurring PSF and additive noise terms from the distorted image and then use those values to deconvolve the distorted image *i(x,y)* using the Wiener filter approach. This is done in an attempt to restore the distorted image as closely as possible to the undistorted image *f(x,y).* A full restoration is impossible as the blurring PSF contains areas of zeros in the high frequency range where the information is completely obliterated. This coupled with other factors, such as quantization noise, means that a perfect restoration is not possible but much of the suppressed information can hopefully be recovered [4, 5, 6].

III. BLUR DETECTION

The first step in the blind deconvolution algorithm is to identify the blur PSF that produced the distorted image. We make use of a novel blur identification approach that we proposed in [12]. The technique starts with an input image which is assumed to contain a Gaussian blur which is described by the following convolution.

$$I = F \otimes G\left(\sigma_1^2\right), \quad (3)$$

Where I is the input image, F is the image without the blur and the function G is a Gaussian kernel with a standard deviation of σ_1. The algorithm will then proceed to attempt to identify the standard deviation of the blur with no other *a priori* information about the contents of the image.

The algorithm constructs a scale-space representation of the input image I. This representation is produced by filtering the input image with a series of Gaussian kernels with ascending values of standard deviation [17]. The series of standard deviations is produced in a similar fashion to the process described in [18]. We start with a standard deviation of 1 and call each doubling of the standard deviation an octave of σ values. We specify how many sub-levels each octave is divided into. The range of σ values is then constructed as described by the pseudo-code in the following figure. This code assumes we want to construct 5 octaves of σ values with 10 divisions in each octave. To construct the scale-space representation D we then convolve the input image with a Gaussian kernel with each of the σ values in the generated range.

```
octaveDivisions = 10
numOfOctaves = 5
scaleFactor = 2.0^(1.0/octaveDivisions)
numOfLevels = octaveDivision*numOfOctaves+1
sigma(1) = 1

For s = 2 to numOfLevels
      Sigma(s) = sigma(s-1)*scaleFactor
end
```

Fig 1: Pseudo-code describing generation of σ values for the scale-space representation

$$D\left(\sigma_2\right) = F \otimes G\left(\sigma_1^2\right) \otimes G\left(\sigma_2^2\right), \quad (4)$$

Where σ_2 is a standard deviation from our generated range and σ_1 is the standard deviation of the original Gaussian PSF we are trying to detect. The next step is to find the absolute error between the input frame and all the images in the scale-space representation.

$$\mathrm{E}(\sigma_2) = \sum \left| F \otimes G\left(\sigma_1^2\right) - F \otimes G\left(\sigma_1^2\right) \otimes G\left(\sigma_2^2\right) \right|, \quad (5)$$

$$\mathrm{E}(\sigma_2) = \sum F \otimes \left| G\left(\sigma_1^2\right) - G\left(\sigma_1^2\right) \otimes G\left(\sigma_2^2\right) \right|, \quad (6)$$

It is shown in [12] that if you plot this error function against the σ_2 values used to construct the scale space D that a point of inflection can be seen at the σ_2 value corresponding to the original blur present in the input image. To find this point of inflection we can analyze the first derivative of the error response E and search for a local extrema which will indicate the detected value for σ_1. Thus once we have the error response for all values of σ_2 in the scale space we can find the first derivative of the error response simply using finite differences.

The final step of the algorithm is to find the first local extrema of *dE/dσ* and the corresponding σ_2 value. This value is the detected standard deviation of the blur that the input image contained. A demonstration of the accuracy of this technique can be found in [12]. This technique is sensitive to additive white Gaussian noise and as such two stages of a 3x3 median filter are applied to the input image *I* to suppress the noise before the blur detection algorithm is run. We found that in images that contain non-uniform blurring such as real-world atmospheric turbulence degraded video that to get reliable points of inflection it was important to only calculate the error from areas of the image which contain real image structures. These areas are detected by calculating the variance in the neighbourhood of each pixel in the image and disregarding the pixels that fall in the lowest 10% of variances found in the image.

IV. NOISE DETECTION

The next step of the blind deconvolution algorithm is to estimate the amount of additive white Gaussian noise present in the input image. The noise is generally assumed to have a zero mean. Detecting additive noise automatically is a challenging task as it is difficult to differentiate between intensity variations in an image that are due to noise and those that are due to real image structures [19, 20, 21, 22].

The approaches to identifying the power of the noise present in an image can be divided into two camps. The first is a block-based approach where the algorithm tries to identify the most homogenous blocks of an image which are assumed to be smooth areas of the image. The intensity variations found in these areas are then considered to be caused by noise and not real image structures. The average variance of these blocks is considered to be a measure of the noise power in an image [20]. Instead of using the average variance of these blocks [21] calculates the mode of the local variances and uses the local variances that occur the most frequently in the image as a measure of the noise power. In [19] colour priors are used to predict what the assumed smooth areas of the image should look like and the residuals between the fitted smooth areas and the real image are used to estimate the noise. All of these methods have the same challenge in that they assume that there are homogenous areas in the image and have to correctly predict the location of these areas.

The second type of approach is a filter-based approach which uses filters to obliterate the coherent information in the image that is due to real structures and leave behind only the noise information. The first algorithm to try this approach was [22] where a Laplacian operator is applied to the image which suppresses the relatively smooth image structures but leaves behind intensity variations caused by noise. This approach works well for high noise levels but because the Laplacian operator also gives a high response on edges it was found that images with a lot of high frequency content were consistently measured as containing high levels of noise. To combat this [23] uses a similar Laplacian operator based approach but also employs an adaptive edge detection step to detect where edges occur in the image and to ignore edge pixels when calculating the variance of the filtered image. The variance of the remaining filtered pixels in the image provides a good measure of the noise power of the image.

To select a method to use in this paper we implemented 3 algorithms from the literature [21, 22, 23] which we will refer to as Mode09, Immerkaer96 and TaiYang08 respectively. We performed an experiment to measure their computational complexity and accuracy at a variety of noise levels. We used a variety of images and added varying strengths of white Gaussian noise to the images and then used the algorithms to detect the strength of the added noise. We performed these experiments using the Monte Carlo method by applying and detecting the noise levels multiple times and computing the average of the detection results. In figure 2 we present the results for detecting noise in the Aircraft test image which had a size of 640x512 pixels. The results presented show the variance of the added noise on the X axis and a ratio of the detected noise to the added noise on the Y axis as described in the equation 7.

$$EstimationRatio = \left| 1 - \frac{\sigma^2_{estimated}}{\sigma^2_{added}} \right| \qquad (7)$$

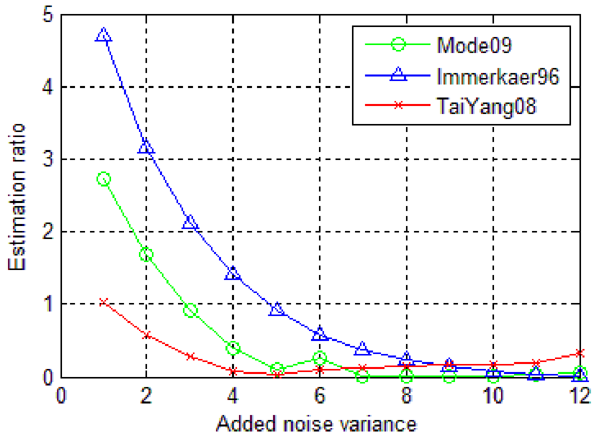

Fig 2: Noise detection accuracy results

In table 1 we list the average processing times of the 3 algorithms for this image on a test PC.

Algorithm	Processing Time
Mode09	2.8906s
Immerkaer96	0.0053s
TaiYang08	0.1199s

Table 1: Average processing times of noise detection algorithms

We can see that the filter-based approaches are far less computationally intensive than block-based approach and as can be seen from the results the accuracy achieved by the approach proposed in TaiYang08 is far more accurate than the block-based approach proposed in Mode09 at low noise levels. At higher noise levels Mode09 does become slightly more accurate but TaiYang08 has the added benefit of executing 26 times faster. We do see that at high noise levels TaiYang08 tends to become less accurate because larger portions of the image are disregarded in the adaptive edge detection step but the majority of images that our blind deconvolution algorithm will be applied to will have noise variances below 5 where TaiYang08 is clearly the most accurate. Based on these results we chose to make use of TaiYang08 in our work. The TaiYang08 algorithm builds on the concepts proposed in Immerkaer96. The Immerkaer96 algorithm first applies a Laplacian operator to the image, the Laplacian kernel used is given in equation 8.

$$L = \begin{bmatrix} 1 & -2 & 1 \\ -2 & 4 & -2 \\ 1 & -2 & 1 \end{bmatrix} \quad (8)$$

This kernel obliterates the majority of the smooth structures in the image leaving only variations caused by noise and sharp edges. Immerkaer96 then calculates the average standard deviation of the noise using equation 9.

$$\sigma_n = \sqrt{\frac{\pi}{2}} \frac{1}{6(W-2)(H-2)} \sum \left| I(x,y) * L \right| \quad (9)$$

where W is the width of the image and H the height. TaiYang08 extends this algorithm by adding in an adaptive edge detection step. The first stage of the edge detection algorithm is to apply the Sobel operator in the X and Y directions. The magnitude of the directional edge responses is summed to provide an absolute edge response. A threshold is then calculated such that 15% of the image is considered to be edges which is a value empirically chosen based on experiments with a series of real world images. The thresholded edge map is then used to exclude edge pixels from the calculation of the average standard deviation given in equation 9.

V. FINAL ALGORITHM FORMULATION

To apply the Wiener filtering approach to a given image we have to estimate a number of quantities to construct the Wiener filter. In section III we showed our technique for estimating the PSF of the blur from the distorted input image. In section IV we showed the technique used to measure the noise present in the distorted image *I*. We however are still missing one quantity to construct the Wiener filter as described in equation 2 and that is the power of the undistorted image signal *F*. We have estimated the power of the additive noise and we can calculate the power of the distorted image signal and from these quantities we estimate the power of the undistorted image. We do this by making the assumption that the noise and undistorted image are not correlated in any way. As such the power of the distorted input image can be viewed as the sum of the power of the undistorted image and the additive noise. We thus use the following equation to estimate the noise-to-signal ratio (NSR) of the input image using the power of the distorted image *I* and the power of the noise.

$$\mathrm{NSR} = S_N/(S_I - S_N) \quad (10)$$

We make one final modification to the classic Wiener filtering approach in our blind deconvolution algorithm. We found that even when you managed to estimate the NSR extremely accurately the Wiener filtering process produces a sharp image in terms of information content where much of the high frequency information has been reconstructed. However the output does not always appear to be of a good quality to a human observer as much of the high frequency elements in the image, edges and texture, appears to be over sharpened and noisy. This is why in many formulations of the Wiener filtering approach the NSR element of the equation is used as a scalar tuning factor and is tweaked manually for each image the process is applied to [5, 6]. We empirically found that if we multiply the NSR by a factor of 10 we achieve a good balance between sharpening and smoothness while taking into account the noise levels in any given image. Wiener filtering is also known to produce extreme ringing artifacts at the image boundaries which are not avoidable. Rather than retain these noisy boundaries we opted to blend the boundaries from the original image into the output images. While the boundaries are thus not deblurred they contain more useful information than the boundary artifacts themselves.

VI. RESULTS

To evaluate the effectiveness of the proposed blind deconvolution scheme we performed 2 experiments. The first experiment started with an unblurred test image we shall refer to as *Aircraft* which has a resolution of 1280x1024. The aircraft test image was then synthetically blurred with a Gaussian kernel of varying standard deviations. After the image was blurred additive white Gaussian noise was added to the image to result in a signal-to-noise ratio of 40 dB. Finally the image was resampled so the intensities are represented by 8-bit values to represent typical quantization noise of digital images.

The blind deconvolution scheme was then run on these test images. The standard deviation of the applied blur was estimated and the amount of noise present was estimated. This information was then used to perform the deconvolution. The results of the algorithm for the test image blurred with a Gaussian blur with a standard deviation of 3 can be seen in figure 3. As can be seen the blur and noise levels were correctly identified and the image that results from the deconvolution is significantly sharper than the input image. The high frequency information was successfully reconstructed while not resulting in unacceptable levels of noise amplification. The ringing artifacts that are usually seen at the borders of the image have been blended out to rather be replaced with samples from the original image as they are more useful to a viewer than the artifacts.

In figures 5 and 6 we can see the results of applying the algorithm to real-world images blurred by atmospheric turbulence. It can be seen that the algorithm sharpens the images with no *a priori* information and does not result in high levels of noise amplification. The images shown in figures 5 and 6 are real-world images and as such do not contain an easy to detect uniform blur. This demonstrates the ability of the algorithm to be effective even when faced with a complex image with a non-uniform blur and still be able to reconstruct the high-frequency content of the image resulting in the restoration of useful image information.

Fig 3 (a)

Fig 3 (b)

Fig 3: (a) Aircraft image with a synthetic Gaussian blur with a σ of 3 and 40db of AWGN (b) result after being deconvolved using the proposed method.

VII. CONCLUSION

This paper presents an algorithm which performs blind-deconvolution on images that have been blurred with a Gaussian blur. This deconvolution is performed using a Wiener filtering based scheme. A novel method is presented to detect the nature of the Gaussian blur contained in an image with no *a priori* information. A number of noise identification algorithms are discussed. The experimental process used to select the noise identification method used in this work is presented. The blur and noise identification schemes are used to estimate their respective quantities from a single image and perform the deconvolution to restore high frequency information that is lost during blurring. Finally the method is applied to a series of test images to demonstrate its effectiveness as an image restoration algorithm.

REFERENCES

[1] S. Winkler, Digital video quality, Wiley, 2005.

[2] H.R. Wu, K.R. Rao, Digital Video Image Quality and Perceptual Coding, CRC Press, 2005.

[3] S.J. Reeves, R.M. Mersereau, “Blur Identification by the method of Generalized Cross-Validation”, IEEE Transactions of Image Processing, Vol. 1, No. 3, 1992.

[4] R.C Puetter, T.R. Gosnell, A. Yahil, “Digital Image Reconstruction: Deblurring and Denoising”, Annual Review of Astronomy and Astrophysics, Vol. 43, pp 139-194, 2005.

[5] R.L. Lagendijk, J. Biemond. “Basic Methods for Image Restoration and Identification” in Handbook of Image and Video Processing. A. Bovik, San Diego: Academic Press, 2000, pp 125-139.

[6] R.C. Gonzales and R.E. Woods, *Digital Image Processin,* Third Edition, Pearson Prentice Hall, 2008, pp. 351-256.

[7] A. K. Katsaggelos, Digital Image Restoration. Springer-Verlag, 1991.

[8] N. Joshi, C.L. Zitnick, R. Szeliski, D.J. Griegman, “Image deblurring and denoising using color priors”, Proceedings of CVPR. 2009, pp. 1550-1557, 2009.

[9] A. Raj and R. Zabih. A graph cut algorithm for generalized image deconvolution. In ICCV ’05, pages 1048–1054, 2005.

[10] Y. Harikumar, G. Bresler. Exact image deconvolution from multiple FIR blurs. IEEE TIP, 8(6):846–862, 1999.

[11] S.C. Park, M.K, Parl M.G. Kang, "Super-Resolution image reconstruction: a techinical overview", IEEE Signal Processing Magazine, Vol 20, Issue 3, pp 21-36, 2003.

[12] P.E. Robinson, Y. Roodt, A. Nel, "Gaussian blur identification using scale-space theory", Proceedings of the Annual Symposium of the Pattern Recognition Association of South Africa (PRASA), In Press, 2012.

[13] A. Levin, Y. Weiss, F. Durand, W.T. Freeman, "Understanding and evaluating blind deconvolution algorithms," Computer Vision and Pattern Recognition (CVPR), vol., no., pp.1964-1971, 20-25 June 2009.

[14] D. Krishnan, T. Tay, R. Fergus , "Blind deconvolution using a normalized sparsity measure," Computer Vision and Pattern Recognition (CVPR), pp.233-240, 20-25 June 2011.

[15] A. K. Katsaggelos and K. T. Lay. "Maximum likelihood blur identification and image restoration using the em algorithm", IEEE Trans. Signal Processing, 1991..

[16] D. Kundur, D. Hatzinakos,, "Blind image deconvolution," Signal Processing Magazine, IEEE , vol.13, no.3, pp.43-64, 1996.

[17] T. Lindeberg, “Scale-space theory: A basic tool for analysing structures at different scales”, Journal of Applied Statistics, vol 21, no. 2, pp 225-270, 1994.

[18] D.G. Lowe, "Distinctive image features from scale-invariant keypoints," International Journal of Computer Vision, Vol. 60, No. 2, pp. 91-110, 2004.

[19] C. Liu, W.T. Freeman, R. Szeliski and S.B. Kang, "Noise estimation from a single image", IEEE Conference on Computer Vision and Pattern Recognition (CVPR), pp. 901-908, 2006.

[20] Amer, E. Dubois, "Fast and Reliable Structure-Oriented Video Noise Estimation", IEEE Transactions on Circuits and Systems for Video Technology, Vol. 15 (1), pp. 113-118, 2005.

[21] S. Aja-Fernández, G. Vegas-Sánchez-Ferrero, M. Martín-Fernández, C. Alberola-López, "Automatic noise estimation in images using local statistics. Additive and multiplicative cases", Image and Vision Computing, Vol. 27 (6), pp 756-770, 2009.

[22] J. Immerkaer, "Fast Noise Variance Estimation", Computer Vision and Image Understanding, Vol.64, No. 2, pp. 300-302, 1996.

[23] S.C. Tai, S.M. Yang, "A fast method for image noise estimation using Laplacian operator and adaptive edge detection", International Symposium on Communications, Control and Signal Processing, pp 1077-10

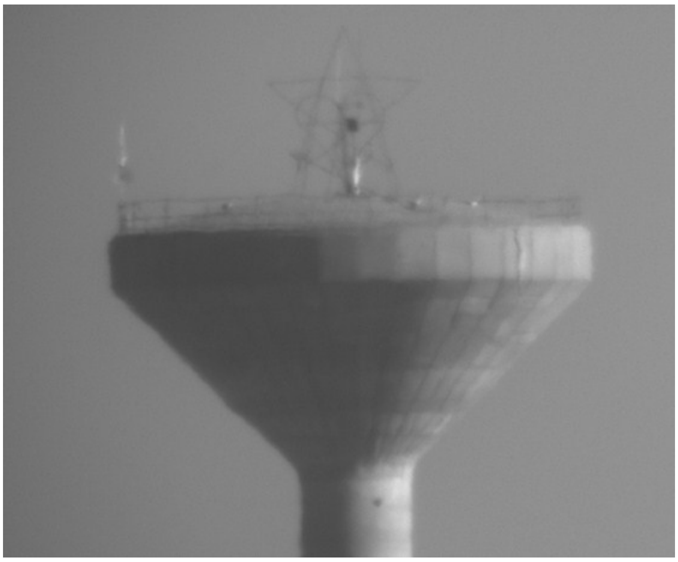

(a)

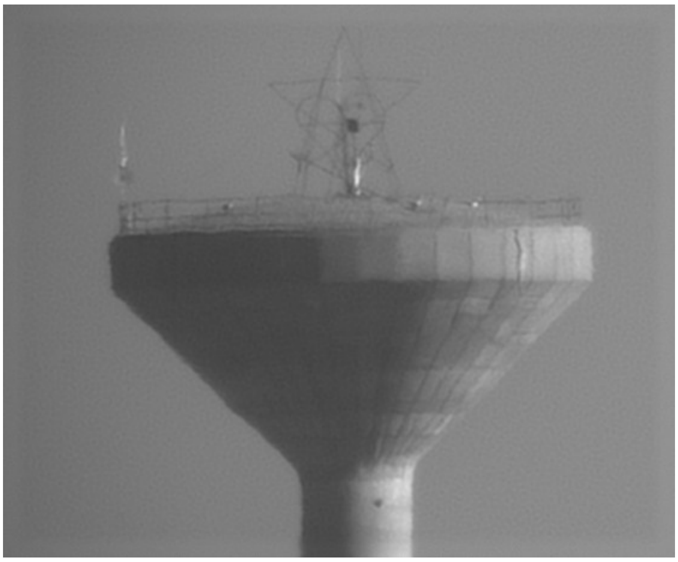

(b)

Fig 5: (a) Real world image containing atmospheric turbulence degradation (560x460) b) result after being deconvolved using the proposed method.

(a)

(b)

Fig 6: (a) Real world image containing atmospheric turbulence degradation 500x750 (b) deconvolved using the proposed method